Hindawi
International Journal of Antennas and Propagation
Volume 2021, Article ID 6680566, 9 pages
https://doi.org/10.1155/2021/6680566

Research Article

2D-OPC Subarray Structure for Efficient Hybrid Beamforming over Sparse mmWave Channels

Junhyuk Yoo,[1] Wonjin Sung ,[1] and In-Kyung Kim[2]

[1]*Department of Electronic Engineering, Sogang University, Seoul 04107, Republic of Korea*
[2]*DISH Wireless, Littleton, CO 80120, USA*

Correspondence should be addressed to Wonjin Sung; wsung@sogang.ac.kr

Received 23 December 2020; Accepted 5 June 2021; Published 15 June 2021

Academic Editor: Raffaele Solimene

Millimeter-wave (mmWave) communication is a key technology of 5G new radio (NR) mobile communication systems. Efficient beamforming using a large antenna array is important to cope with the significant path loss experienced in the mmWave spectrum. The existing fully digital beamforming scheme requires a separate radio frequency (RF) chain for each antenna, which results in an excessive hardware cost and consumption power. Under these circumstances, hybrid beamforming which approaches the performance of fully digital beamforming while reducing the complexity is a promising solution for the mmWave multiuser transmission. By extending the existing hybrid beamforming strategies, this paper proposes a novel architecture which effectively reduces the hardware cost and complexity for large antenna arrays. The proposed scheme includes multiple subarrays in the form of uniform planar array (UPA) which are allowed to be overlapped in the two-dimensional space. The corresponding antenna structure is referred to as the two-dimensional overlapped partially connected (2D-OPC) subarray structure. We evaluate the performance of the proposed scheme to suggest performance-complexity trade-offs in designing versatile antenna arrays for efficient beamforming over the mmWave channel.

1. Introduction

The key techniques adopted by the fifth-generation (5G) wireless systems include the utilization of higher frequency bands to significantly increase the transmitted data rates using enlarged bandwidth resources [1, 2]. Due to the shortage of frequency resources in conventional low frequency bands, the utilization of the millimeter-wave (mmWave) spectrum is actively pursued [3–5]. The mmWave communication can transmit gigabit data per second but suffer from high path loss and low scattering [6, 7]. To overcome these difficulties, large antenna arrays need to be applied in mmWave communication systems to perform high-gain beamforming. The short wavelength, one of the features of mmWave communication, enables a large number of antennas to be packed within a limited space. This results in high directional beamforming gains, which compensates for the severe path loss.

In multiple-input multiple-output (MIMO) systems using a large-scale antenna array, conventional digital beamforming requires a separate radio frequency (RF) chain for each antenna element. This causes high power consumption as well as high hardware cost, which makes both the operation cost and capital expenditures increase [8, 9]. Investigations have been made to suggest various architectures aimed at reducing the number of RF chains by using the separate analog RF beamformer and baseband digital beamformer, known as the hybrid beamforming technique [10–12]. Unlike conventional digital beamforming, hybrid beamforming is performed by using phase shifters in the analog RF domain. Analog beamforming controls the direction of the signal by adjusting the phase shifters, with much lower complexity compared with digital beamforming. Performance degradation is experienced, however, due to the lack of precise signal processing capability at the baseband, including the lack of the controllability of the magnitude of the beamformer coefficients.

In general, two hybrid beamformer structures are usually adopted. These are, respectively, the fully connected structure (FCS) [13–15] and the partially connected structure (PCS) [16–19]. The FCS can achieve the full array gain because each RF chain is connected to all antennas, but it is not practically efficient because it requires a large number of phase shifters and power amplifiers. On the other hand, each RF chain in the PCS is connected to a group of antenna elements called a subarray. The PCS effectively reduces the number of phase shifters required, decreasing the beamforming gain of each RF chain in return.

In order to implement the mmWave hybrid beamforming architecture that achieves high beamforming gain while minimizing the number of phase shifters required, there have been some attempts to generalize the antenna structure including the possible overlaps among subarrays. Most of the existing overlapped subarray structures (OSSs), however, are based on one-dimensional uniform linear arrays (ULAs) [20, 21] or targeted to single-user transmission environments [22]. In this paper, we generalize the overlapping structure using the UPAs to propose the two-dimensional overlapped partially connected (2D-OPC) subarray structure that can support various subarray shapes. Each antenna element can be connected to either single or multiple RF chains to provide versatility in the utilization of subarrays. The 2D-OPC structure can reduce the required number of phase shifters while maintaining the data throughput performance. The proposed subarray structure includes both the FCS and PCS as special cases. The rest of the paper is organized as follows. In Section 2, signal and channel models are described. The 2D-OPC subarray structure is discussed in Section 3, followed by the performance evaluation results in Section 4. Conclusions are given in Section 5.

2. System Model

We consider a mmWave multiuser MIMO communication system. User equipments (UEs) are randomly distributed in hexagonal cells as shown in Figure 1, located at the height of h_{UE} from the ground. The base station (BS) is equipped with M transmit antennas which are connected to N_{RF} RF chains and performs simultaneous transmission to K UEs. The height of the BS antenna is denoted by h_{BS}. The beamforming module consists of the analog beamformer $\mathbf{F}_{\mathrm{RF}} \in \mathbb{C}^{M\times K}$ and the digital beamformer $\mathbf{F}_{\mathrm{BB}} \in \mathbb{C}^{K\times K}$. The transmitted signal vector $\mathbf{x} \in \mathbb{C}^{K\times 1}$ from the antenna array can then be expressed as $\mathbf{x} = \mathbf{F}_{\mathrm{RF}}\mathbf{F}_{\mathrm{BB}}\mathbf{s}$, where $\mathbf{s} \in \mathbb{C}^{K\times 1}$ represents the transmitted symbol containing K data streams in the baseband with $\mathbb{E}[\mathbf{s}\mathbf{s}^H] = \mathbf{I}_K$. At the receiver, the received signal $\mathbf{y} \in \mathbb{C}^{K\times 1}$ is written as.

$$\mathbf{y} = \mathbf{H}\mathbf{F}_{\mathrm{RF}}\mathbf{F}_{\mathrm{BB}}\mathbf{s} + \mathbf{n}, \tag{1}$$

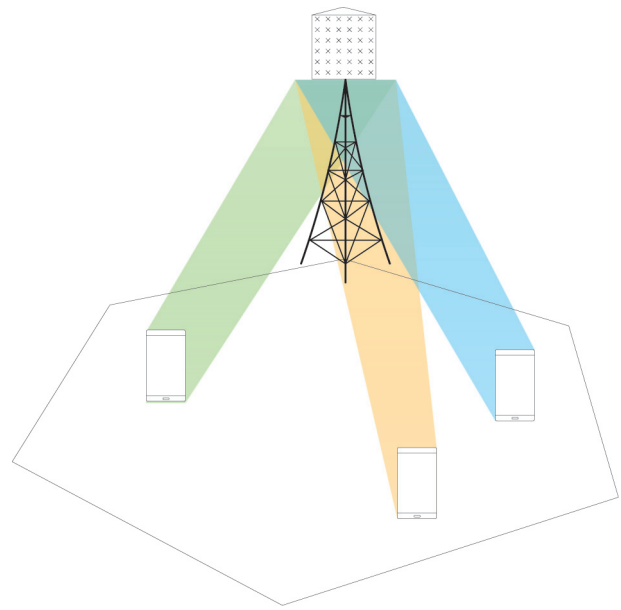

Figure 1: A MU-MIMO system with a large-scale antenna array.

where $\mathbf{H} \in \mathbb{C}^{K\times M}$ is the channel matrix and $\mathbf{n} \sim CN(0, \sigma^2\mathbf{I}_K)$ is the $K \times 1$ Gaussian noise vector including independent identically distributed (i.i.d.) complex Gaussian variables. We assume that all UEs have the identical noise variance σ^2. The achievable rate R_k for the k th UE can be expressed using the received signal-to-noise ratio (SNR) as

$$R_k = \log_2\left(1 + \frac{\left|\mathbf{h}_k^T\mathbf{F}_{\mathrm{RF}}\mathbf{f}_k^{\mathrm{BB}}\mathbf{s}_k\right|^2}{\sum_{i\neq k}^{K}\left|\mathbf{h}_k^T\mathbf{F}_{\mathrm{RF}}\mathbf{f}_{\mathbf{i}}^{\mathrm{BB}}\mathbf{s}_i\right|^2 + \sigma^2}\right), \tag{2}$$

where $\mathbf{f}_{\mathbf{i}}^{\mathrm{BB}}$ is the $K \times 1$ i-th column of the digital beamformer $\mathbf{F}_{\mathrm{BB}}$. Sum-rate R of the system can be represented as $R = \sum_{k=1}^{K} R_k$.

We consider a $V \times H$ uniform planar array (UPA) with M antennas as the overall BS antenna structure, which includes multiple subarrays. The 2D-OPC subarray structure is shown in Figure 2, where the subarray has v vertical elements and h horizontal elements, i.e., the subarray has $p = vh$ antennas. When the size of each subarray is identical to the overall antenna array, i.e., $v = V$ and $h = H$, the corresponding structure becomes the FCS by connecting the full-size subarray of size $p = M$ to each of N_{RF} RF chains. When subarrays in utilization partition the overall array, i.e., each subarray has $p = (M/N_{\mathrm{RF}})$ antennas, the corresponding structure becomes the PCS by connecting each subarray to a single RF chain. The normalized array response vector of a UPA in the direction with azimuth angle ϕ and zenith angle θ is written as.

$$\mathbf{a}(\phi,\theta) = \frac{1}{\sqrt{M}}\left[1, \ldots, e^{j(2\pi/\lambda)\mathrm{d}(m\sin\phi\sin\theta + n\cos\theta)}, \ldots, e^{j(2\pi/\lambda)\mathrm{d}((H-1)\sin\phi\sin\theta + (V-1)\cos\theta)}\right]^T, \tag{3}$$

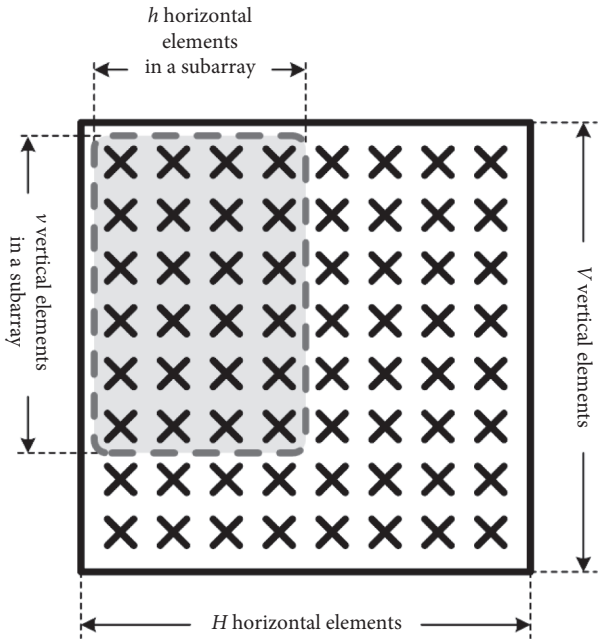

Figure 2: A uniform planar array including subarrays for hybrid beamforming.

where $m = 0, 1, \ldots, H-1$ is the horizontal antenna index and $n = 0, 1, \ldots, V-1$ is the vertical antenna index. Also, λ is the signal wavelength and d is the spacing between two adjacent antenna elements. Since the mmWave propagation environment is well characterized by the channel model with limited scattering [23], we adopt a simplified clustered channel model, i.e., the Saleh–Valenzuela (S-V) model in [24]. The $K \times M$ channel matrix $\mathbf{H}$ under the S-V model can be written as follows [25]:

$$\mathbf{H} = \left[\mathbf{h}_1, \mathbf{h}_2, \ldots, \mathbf{h}_K\right]^T, \tag{4}$$

where

$$\mathbf{h}_k^H = \sqrt{\frac{M}{L}} \sum_{l=1}^{L} \boldsymbol{\alpha}_{k,l} \mathbf{a}^H\left(\phi_{k,l}, \theta_{k,l}\right). \tag{5}$$

The k-th UE channel matrix $\mathbf{h}_k$ has average power equal to the total number of antennas, i.e., $\mathbb{E}[\mathbf{h}_k^H \mathbf{h}_k] = M$, where L represents the number of propagation paths between BS and UE. It is assumed that each scatterer contributes to a single propagation path, with complex gain coefficient $\alpha_{k,l}$ for the l-th path for the k-th UE. The coefficient is modelled to follow the complex Gaussian distribution, i.e., $\alpha_{k,l} \sim CN(0, 1)$. Parameter $\phi_{k,l}$ denotes the azimuth angle of arrival for the l-th path which follows the Laplacian distribution with mean ϕ_k and variance σ_ϕ^2. Also, $\theta_{k,l}$ denotes the zenith angle of arrival for the l-th path which follows the Laplacian distribution with mean θ_k and variance σ_θ^2. Another channel model of interest in this paper is the three-dimensional spatial channel model (3D-SCM) described in [26]. The 3D-SCM includes the propagation information for carrier frequency bands in the range of 0.5 GHz to 100 GHz. Statistical properties of radio propagation in this frequency range including the delay spread, angular spreads, Ricean K factor, and shadow fading are all captured by parameters applied to this model. The channel matrix in equation (4) can be generated according to this model to support different transmission scenarios such as urban macrocell (UMa), urban microcell (UMi), rural macrocell (RMa), and indoor hotspot (InH).

3. 2D Overlapped Partially Connected Subarray Structure

In the FCS, each antenna element is connected to all RF chains. Taking advantage of a network that is fully connected between the antenna elements and the RF chains, the FCS can achieve the full beamforming gain for each RF chain. However, the FCS requires a substantial number of power amplifiers and phase shifters which makes its practical implementation less attractive. The number of required phase shifters is as many as MN_{RF}. For the PCS, the whole array is divided into disjoint subarrays, and the antenna elements in each subarray are connected to a single RF chain. The total number of phase shifters in this case is M, significantly reducing the hardware complexity. Despite this complexity reduction, the utilization of the PCS is limited due to the degraded transmission performance.

In order to solve the weaknesses of the existing hybrid beamforming, the OSS was introduced to achieve a higher beamforming gain while maintaining the hardware complexity at a reasonable level. The 2D-OPC subarray structure is a generalization of the OSS for the ULA to the planer 2D space. Each subarray in the 2D-OPC structure is connected to multiple RF chains and can overlap in both horizontal and vertical directions with other subarrays. The proposed the 2D-OPC subarray structure is shown in Figure 3. The set of antenna indices included in the subarray connected to the k-th RF chain is defined as.

$$I_k = \left\{i_1, i_2, \ldots, i_p\right\}, \tag{6}$$

which includes $p = vh$ elements. In Figure 3, $c_{k,m}$ is the parameter indicating whether the m-th antenna element is connected to the k-th RF chain and is defined as

$$c_{k,m} = \begin{cases} 1, & \text{if } m \in I_k, \\ 0, & \text{if } m \notin I_k. \end{cases} \tag{7}$$

If $c_{k,m} = 1$, the k-th RF chain and the m-th antenna are connected with a phase shifter. If $c_{k,m} = 0$, on the other hand, the k-th RF chain and the m-th antenna are not connected, and no phase shifter exists. We assume there are S subarrays, each including $p = vh$ antenna elements. We further allow one subarray being connected q different RF chains, with index sets satisfying $I_1 = I_2 = \cdots = I_q$, for example. Parameter q is called the multiplicity factor for subarrays. Accordingly, the total number of RF chains satisfies $N_{\mathrm{RF}} = qS$ and the total number of phase shifters satisfies $N_{\mathrm{PS}} = pN_{\mathrm{RF}} = pqS$. As a special case, the FCS has index sets $I_k = \{1, 2, \ldots, M\}$ for $k = 1, 2, \ldots, N_{\mathrm{RF}}$, and multiplicity factor is $q = N_{\mathrm{RF}}$. In Figure 4(a), $S = 4$ subarrays of size $v = 6$ and $h = 6$ are located in the overall array of size $V = 8$ and $H = 8$ in an overlapped fashion. Each subarray is connected

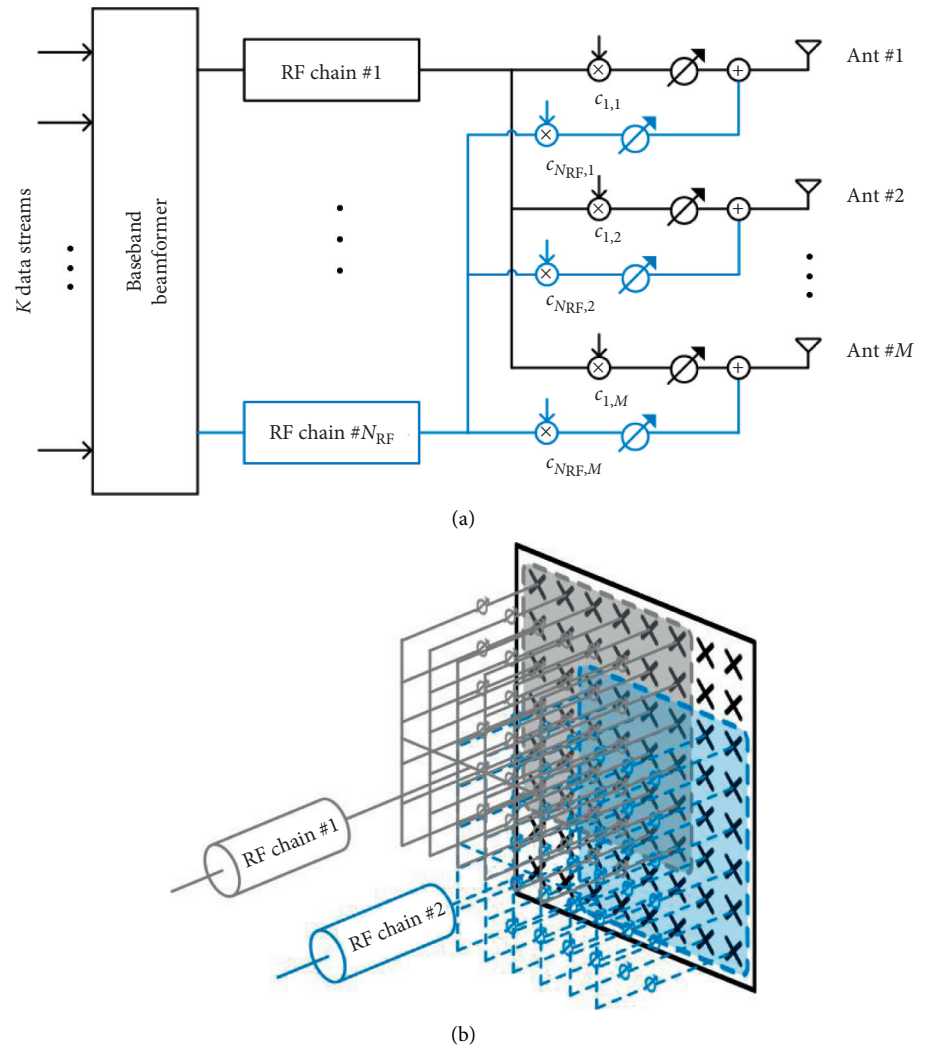

FIGURE 3: Two-dimensional overlapped partially connected subarray structure: (a) RF chain connection; (b) $v = 6$ and $h = 6$ subarray example.

to one of 4 RF chains in the antenna structure when multiplicity factor is $q = 1$. In Figure 4(b), $S = 3$ subarrays of size $v = 8$ and $h = 4$ are placed in the overall array. The number of RF chains is $N_{RF} = S = 3$ if the multiplicity factor is $q = 1$. If the multiplicity factor is $q = 2$, two RF chains are connected to the same subarray with separate sets of phase shifters, and the total number of RF chains in use becomes $N_{RF} = qS = 6$. By changing the subarray size, the number of subarrays, and the multiplicity factor, various different ways of constituting the antenna arrays can be arranged, providing a significantly increased degree of freedom in array design.

$$\mathbf{F}_{RF} = [\mathbf{f}_1, \mathbf{f}_2, \ldots, \mathbf{f}_K], \tag{8}$$

Hybrid beamforming is performed in two steps. First, analog beamformer $\mathbf{F}_{RF}$ is applied using RF phase shifters with the constant modulus constraint on beamforming elements. The $M \times K$ analog beamformer is constructed as follows.where $\mathbf{f}_k = [f_{k,1}, f_{k,2}, \ldots, f_{k,M}]^T$ is the $M \times 1$ analog beamforming vector for the k-th UE with its elements defined as

$$f_{k,m} = \begin{cases} \dfrac{1}{\sqrt{P}} \dfrac{\left[\mathbf{H}^H\right]_{k,m}}{\left|\left[\mathbf{H}^H\right]_{k,m}\right|}, & \text{if } m \in \mathrm{I}_k, \\ 0, & \text{if } m \notin \mathrm{I}_k, \end{cases} \tag{9}$$

for $k = 1, 2, \ldots, K$ and $m = 1, 2, \ldots, M$. Here, $[.]_{m,n}$ denotes the (m, n)-th element of a matrix. Secondly, the digital beamformer is determined. For example, the zero-forcing (ZF) precoder can be applied to the effective channel $\mathbf{H}_{eff} = \mathbf{H}\mathbf{F}_{RF}$ to eliminate the multiuser interference. The dimension for the effective channel is $K \times K$, obtained by multiplying the $K \times M$ channel $\mathbf{H}$ and $M \times K$ analog beamformer $\mathbf{F}_{BB}$. In this case, the $K \times K$ digital beamformer has the form of

$$\mathbf{F}_{BB} = \mathbf{H}_{eff}^H \left(\mathbf{H}_{eff}\mathbf{H}_{eff}^H\right)^{-1}. \tag{10}$$

For equal power allocation to all users, the column-wise power normalization may be applied to the overall beamformer $\mathbf{F} = \mathbf{F}_{RF}\mathbf{F}_{BB}$. The dimension for the overall

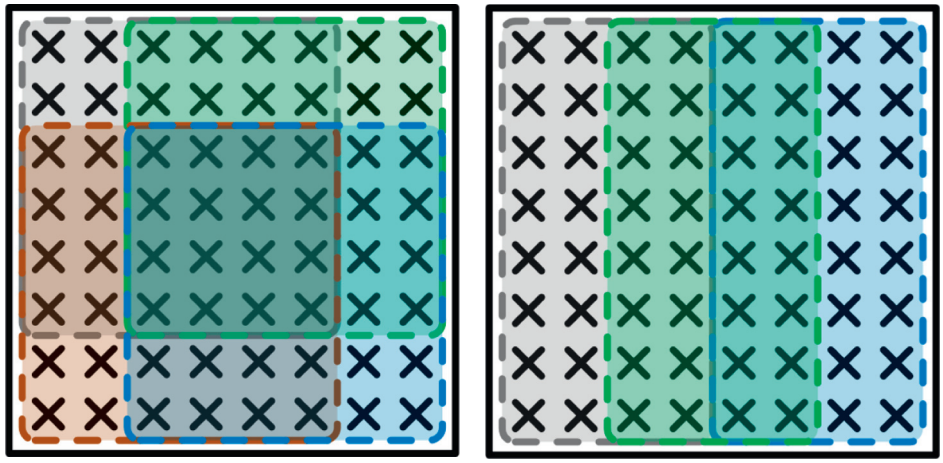

(a) (b)

Figure 4: Illustration of 2D-OPC subarray structures: (a) $v = 6$ and $h = 6$; (b) $v = 8$ and $h = 4$.

beamformer is $M \times K$, obtained by multiplying the $M \times K$ analog beamformer $\mathbf{F}_{\text{RF}}$ and $K \times K$ digital beamformer $\mathbf{F}_{\text{BB}}$.

4. Performance Evaluation

We present performance evaluation results for the proposed 2D-OPC array structure under different parameter settings. Three types of channel models are used for the evaluation. The first channel of interest is the pure line-of-sight (LoS) channel with $L = 1$ single path. The second channel is based on the multipath S-V model with $L = 8$ paths. The azimuth and zenith angles for each path follow the Laplacian distribution with mean values ϕ_k and θ_k determined according to the UE's location, which is randomly assigned within the cell with the intersite distance of 200 m. The angular spread of 5° is used for the Laplacian distribution. The third channel model is the SCM UMi adopted by 3GPP for link-level performance evaluation for urban microcells [26]. We first apply the $L = 1$ LoS channel for performance evaluation results in Figures 5–8 and then extend the evaluation to all channel models in Figures 9–11. UEs are assumed to have a single antenna. The antenna heights for the BS and the UEs are, respectively, $h_{BS} = 10$ m and $h_{\text{UE}} = 1.5$ m. Unless otherwise stated, the received signal-to-noise (SNR) at the UEs is assumed to be 20 dB.

The UPA at the BS has $M = 64$ antennas with $V = 8$ vertical elements and $H = 8$ horizontal elements. Although the 2D-OPC array structure of any sizes can be used for proposed hybrid beamforming, we choose the 8×8 UPA for the performance verification. The 8×8 UPA is an array type adopted by the 5G NR standard, as specified in 3GPP TR 38.901 [26]. Many other related investigation results for hybrid beamforming are given using the array dimension $V = H = 8$ for this reason, including those in [9, 22]. The spacing between adjacent antenna elements is set to be half-wavelength. Subarray dimensions are chosen to be in even numbers $v = 2, 4, 6, 8$ and $h = 2, 4, 6, 8$ which do not exceed

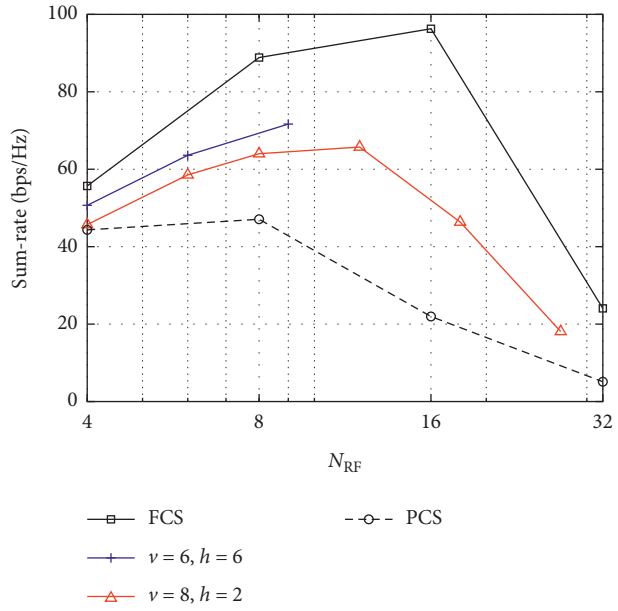

Figure 5: Sum-rate versus the number of RF chains for different antenna structures.

the maximum size of $V = 8$ and $H = 8$. Using these subarray parameters, symmetric placements of subarrays within the whole 8×8 array can be made as further explained below.

Let X denote the number of horizontal shifts and Y denote the number of vertical shifts of the subarrays within the overall antenna array of size V-by-H. The total number of subarrays is determined as $S = XY$. The "anchor point" for each subarray is the two-dimensional index set (a, b) denoting the horizonal and vertical antenna indices for the upper left corner of the v-by-h subarray. We locate the subarrays to have equal spacing between neighbouring subarrays, with the anchor point for the first subarray at (1, 1). The anchor points for all subarrays can be described by.

$$\left(1+\frac{(V-v)}{(Y-1)}(y-1), 1+\frac{(H-h)}{(X-1)}(x-1)\right), \quad (11)$$

for $x = 1, 2, \ldots, X$ and $y = 1, 2, \ldots, Y$. For 2D-OPC arrangements in Figure 5, the anchor points are set as follows:

(1) For $N_{RF} = 4$, (1, 1), (3, 1), (1, 3), (3, 3) with $X = 2$ and $Y = 2$

(2) For $N_{RF} = 6$, (1, 1), (2, 1), (3, 1), (1, 3), (2, 3), (3, 3) with $X = 3$ and $Y = 2$

(3) For $N_{RF} = 9$, (1, 1), (2, 1), (3, 1), (1, 2), (2, 2), (3, 2), (1, 3), (2, 3), (3, 3) with $X = 3$ and $Y = 3$.

We first evaluate the sum-rate versus the number of RF chains and present the corresponding result in Figure 5. Each RF chain is connected to a single subarray with multiplicity factor $q = 1$ in this figure. As can be seen in the figure, the sum-rate performance for all array structures tend to increase as the number RF chains increases. After the number of RF chains exceeds 16, however, interuser interference becomes more severe to overcompensate the spatial multiplexing gain. The sum-rate performance for the 2D-OPC structure significantly exceeds that of the conventional PCS, and the performance improves as the subarray size increases. However, a larger subarray can support a limited number of locational shifts within the overall array, thereby providing a limited range of support for the RF chains. This limitation can be removed by introducing the multiplicity factor, by connecting the same subarray to q RF chains.

Figure 6 shows the sum-rate performance with different multiplicity factors, and it can be observed that a wider range of RF chain numbers can be supported by increasing the value of q. It is also noted from the figure that there exists a value of q which gives the best sum-rate performance for given N_{RF}. Therefore, it is recommended that we use this optimal q value for the 2D-OPC subarray design. The optimal choice of q depends on the subarray sizes, and the figure shows such choices for subarrays with parameters $(v = 6, h = 6)$, $(v = 8, h = 2)$, and $(v = 2, h = 4)$. All subsequent performance figures are based on these optimal values for q.

Although the FCS outperforms the 2D-OPC subarray structure in Figure 5, it uses a significantly larger number of phase shifters due to the full connections to RF chains from each antenna element. Therefore, we compute the number of all phase shifters in use for each array structure for given numbers of RF chains and then present the sum-rate versus the number of phase shifters N_{PS} in Figure 7. The figure exhibits the fact that there exists a certain range of N_{PS} values over which the proposed structure outperforms the conventional FCS. The result can be applied to choose a desirable antenna structure under the constraint of strict limitations on hardware cost.

We further normalize the performance by dividing the achievable sum-rate by the number of phase shifters in use and then plot this normalized sum-rate as a function of N_{RF} in Figure 8. Again, we observe that the proposed scheme can outperform the FCS in this measure, confirming the strong cost-effectiveness of the 2D-OPC structure.

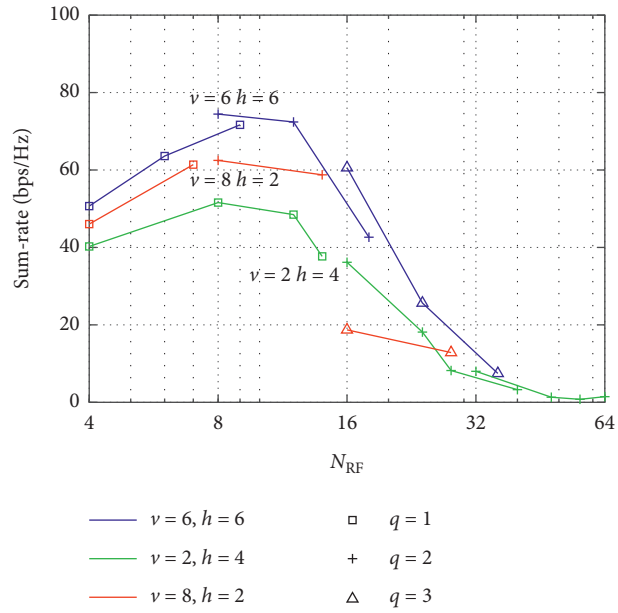

Figure 6: Sum-rate versus the number of RF chains for different multiplicity factors.

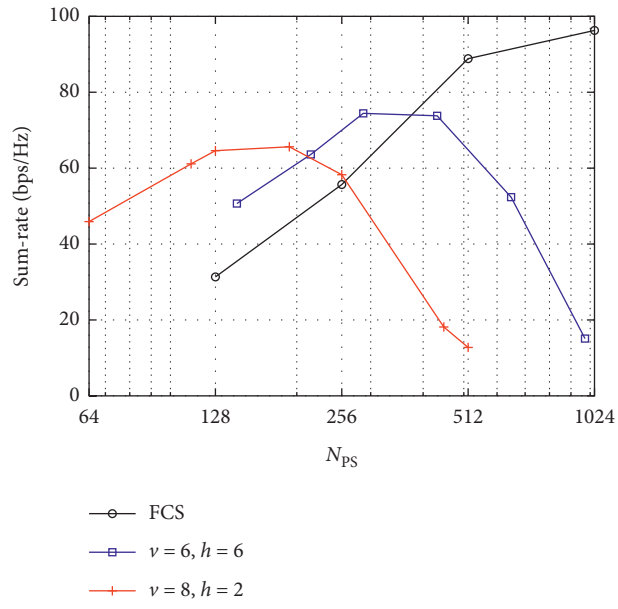

Figure 7: Sum-rate versus the number of phase shifters.

We extend our performance evaluation results to a wider class of channels. In Figures 9 and 10, the sum-rate performance is evaluated and compared for three different types of channel models in consideration. The multipath channel with enhanced spatial diversity exhibits improved throughput performance over LoS channel. On the other hand, the SCM with a large number of clusters and rays within each cluster generates received power fluctuations and reduces the transmission performance.

Figure 11 shows the sum-rate performance for these channel types for increasing values of the signal-to-noise ratio (SNR). The 6-by-6 subarray is used with the number of

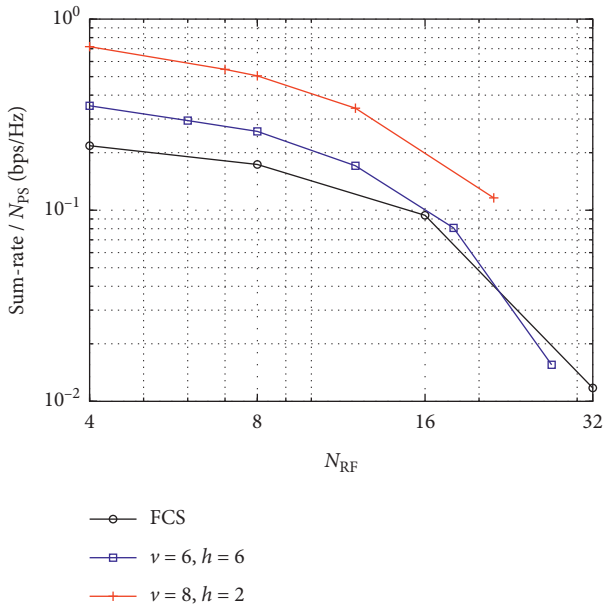

Figure 8: Sum-rate per phase shifter versus the number of RF chains.

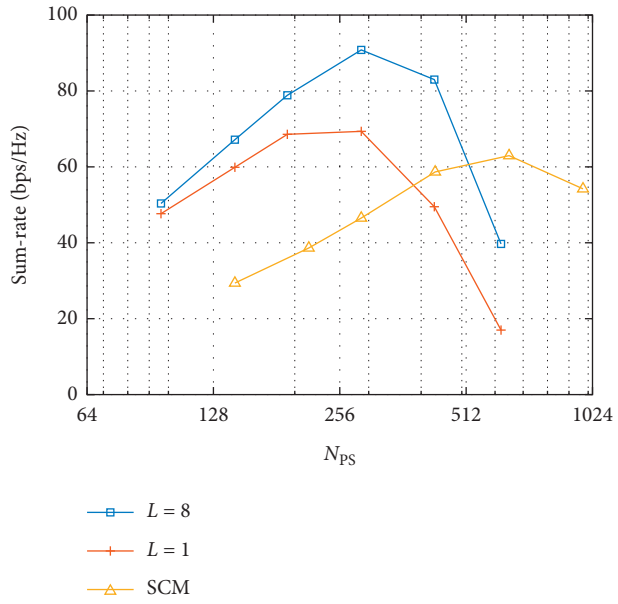

Figure 10: Sum-rate versus the number of phase shifters in different channel environments ($v = 6, h = 6$).

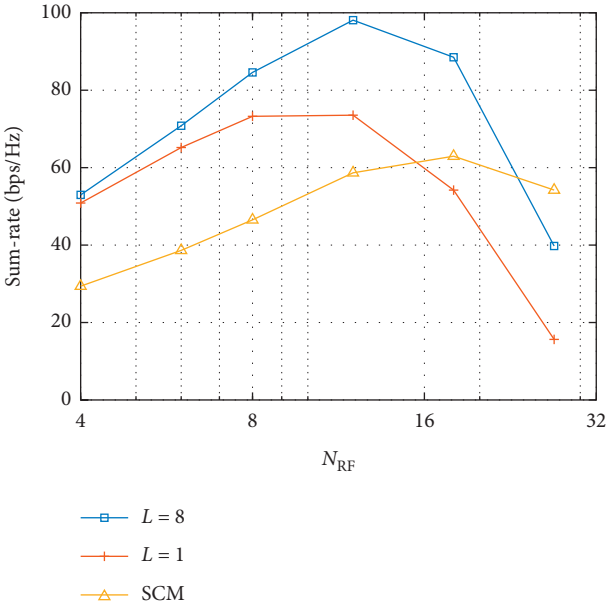

Figure 9: Sum-rate versus the number of RF chains in different channel environments ($v = 6$, $h = 6$).

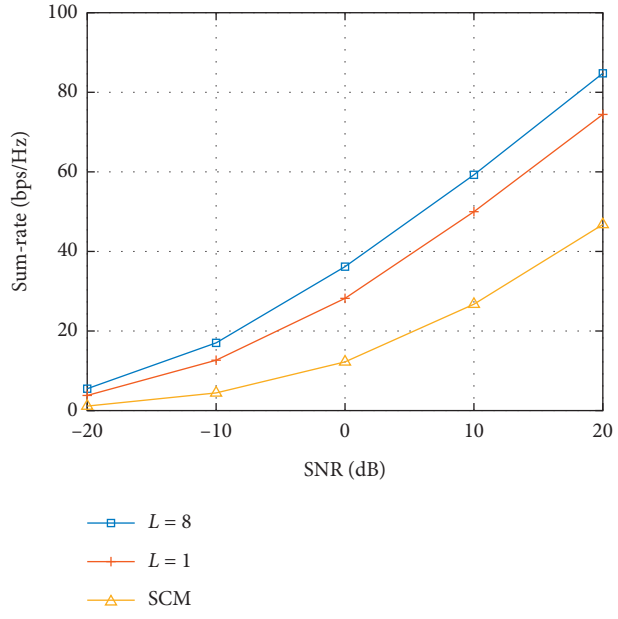

Figure 11: Sum-rate versus the SNR ($N_{RF} = 8, v = 6, h = 6$).

RF chains set to $N_{RF} = 8$ for this evaluation. Finally, Figure 12 lists the sum-rate performance for different subarrays with various sizes over the LoS channel. For each of these subarrays, similar performance comparisons can be made in terms of the multiplicity factor, the number of phase shifters, and normalized sum-rate. The result can be used as a reference in choosing appropriate array parameters for given conditions.

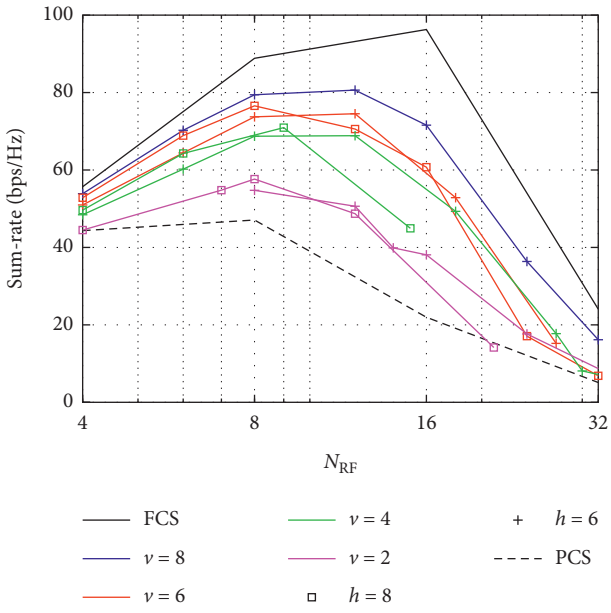

Figure 12: Sum-rate performance of various subarray sizes.

5. Conclusions

We presented a generalized description of the overlapped subarray structure for UPAs, which includes the existing FCS, PCS, and 1D OSS as special cases. By adjusting the parameters for the 2D-OPC subarray structure, the hardware complexity of the overall antenna array can be adequately controlled. Performance evaluation results show that the array parameters which maximize the throughput can be chosen for given conditions such as the supported number of users for simultaneous data transmission, i.e., the number of RF chains employed in the antenna system. A good balance between the hardware cost and the sum-rate performance can be achieved by employing the proposed structure. Although the presented results are mainly targeted for the mmWave channel, the same approach can also be adopted at lower frequencies with a dominant directional path, for which hybrid beamforming effectively applies.

Data Availability

The data used to support this study are available upon request to the authors.

Conflicts of Interest

The authors declare that they have no conflicts of interest.

Acknowledgments

This work was supported by the National Research Foundation (NRF) of Korea and MSIP (no. 2020R1A2C1004135).

References

[1] M. S. Ayub, L. Wuttisittikulkij, P. Adasme, and I. Soto, "Hybrid precoding design for two carriers aggregated in 5G massive MIMO system," in *Proceedings of the 2020 South American Colloquium on Visible Light Communications (SACVC)*, pp. 1–5, Santiago, Chile, June 2020.

[2] R. Zhang, J. Zhou, J. Lan, B. Yang, and Z. Yu, "A high-precision hybrid analog and digital beamforming transceiver system for 5G millimeter-wave communication," *IEEE Access*, vol. 7, pp. 83012–83023, 2019.

[3] S. Han, C.-l. Xu, and C. Rowell, "Large-scale antenna systems with hybrid analog and digital beamforming for millimeter wave 5G," *IEEE Communications Magazine*, vol. 53, no. 1, pp. 186–194, 2015.

[4] N. Li, Z. Wei, H. Yang, X. Zhang, and D. Yang, "Hybrid precoding for mmWave massive MIMO systems with partially connected structure," *IEEE Access*, vol. 5, pp. 15142–15151, 2017.

[5] A. Gupta and R. K. Jha, "A survey of 5G network: architecture and emerging technologies," *IEEE Access*, vol. 3, pp. 1206–1232, 2015.

[6] Z. Pi and F. Khan, "An introduction to millimeter-wave mobile broadband systems," *IEEE Communications Magazine*, vol. 49, no. 6, pp. 101–107, 2011.

[7] M. Xiao, S. Mumtaz, Y. Huang et al., "Millimeter wave communications for future mobile networks," *IEEE Journal on Selected Areas in Communications*, vol. 35, no. 9, pp. 1909–1935, 2017.

[8] F. Sohrabi and W. Yu, "Hybrid digital and analog beamforming design for large-scale antenna arrays," *IEEE Journal of Selected Topics in Signal Processing*, vol. 10, no. 3, pp. 501–513, 2016.

[9] A. Alkhateeb, G. Leus, and R. W. Heath, "Limited feedback hybrid precoding for multi-user millimeter wave systems," *IEEE Transactions on Wireless Communications*, vol. 14, no. 11, pp. 6481–6494, 2015.

[10] I. Ahmed, H. Khammari, A. Shahid et al., "A survey on hybrid beamforming techniques in 5G: architecture and system model perspectives," *IEEE Communications Surveys & Tutorials*, vol. 20, no. 4, pp. 3060–3097, 2018.

[11] J. Zhang, X. Huang, V. Dyadyuk, and Y. Guo, "Massive hybrid antenna array for millimeter-wave cellular communications," *IEEE Wireless Communications*, vol. 22, no. 1, pp. 79–87, 2015.

[12] J. Zhang, X. Yu, and K. B. Letaief, "Hybrid beamforming for 5G and beyond millimeter-wave systems: a holistic view," *IEEE Open Journal of the Communications Society*, vol. 1, pp. 77–91, 2020.

[13] P. Zhao and Z. Wang, "Hybrid precoding for millimeter wave communications with fully connected subarrays," *IEEE Communications Letters*, vol. 22, no. 10, pp. 2160–2163, 2018.

[14] O. El Ayach, R. W. Heath, S. Rajagopal, and Z. Pi, "Multimode precoding in millimeter wave MIMO transmitters with multiple antenna sub-arrays," in *Proceedings of the 2013 IEEE Global Communications Conference (GLOBECOM)*, pp. 3476–3480, Atlanta, GA, USA, December 2013.

[15] L. Dai, X. Gao, J. Quan, S. Han, and I. Chih-Lin, "Near-optimal hybrid analog and digital precoding for downlink mmWave massive MIMO systems," in *Proceedings of the 2015 IEEE International Conference on Communications (ICC)*, pp. 1334–1339, London, UK, June 2015.

[16] M. Majidzadeh, A. Moilanen, N. Tervo, H. Pennanen, A. Tölli, and M. Latva-aho, "Hybrid beamforming for single-user MIMO with partially connected RF architecture," in *Proceedings of the 2017 European Conference on Networks and Communications (EuCNC)*, pp. 1–6, Oulu, Finland, June 2017.

[17] C. Hu, Y. Liu, L. Liao, and R. Zhang, "Hybrid beamforming for multi-user MIMO with partially-connected RF

architecture," *IET Communications*, vol. 13, no. 10, pp. 1356–1363, 2019.

[18] Y. Wang and W. Zou, "Hybrid precoding design for millimetre wave systems with the partially-connected structure," *IET Communications*, vol. 14, no. 4, pp. 561–567, 2020.

[19] M. Zhu, G. Xie, and X. Qi, "Low-complexity partially-connected hybrid precoding for massive MIMO systems," in *Proceedings of the 2020 IEEE Wireless Communications and Networking Conference (WCNC)*, pp. 1–6, Seoul, South Korea, May 2020.

[20] N. Song, T. Yang, and H. Sun, "Overlapped subarray based hybrid beamforming for millimeter wave multiuser massive MIMO," *IEEE Signal Processing Letters*, vol. 24, no. 5, pp. 550–554, 2017.

[21] Z. Wang, J. Zhu, J. Wang, and G. Yue, "An overlapped subarray structure in hybrid millimeter-wave multi-user MIMO system," in *Proceedings of the 2018 IEEE Global Communications Conference (GLOBECOM)*, pp. 1–6, Abu Dhabi, UAE, December 2018.

[22] C.-C. Hu and J.-H. Zhang, "Hybrid precoding design for adaptive subconnected structures in millimeter-wave MIMO systems," *IEEE Systems Journal*, vol. 13, no. 1, pp. 137–146, 2019.

[23] H. Hao Xu, V. Kukshya, and T. S. Rappaport, "Spatial and temporal characteristics of 60-GHz indoor channels," *IEEE Journal on Selected Areas in Communications*, vol. 20, no. 3, pp. 620–630, 2002.

[24] A. M. Sayeed, "Deconstructing multiantenna fading channels," *IEEE Transactions on Signal Processing*, vol. 50, no. 10, pp. 2563–2579, 2002.

[25] O. E. Ayach, S. Rajagopal, S. Abu-Surra, Z. Pi, and R. W. Heath, "Spatially sparse precoding in millimeter wave MIMO systems," *IEEE Transactions on Wireless Communications*, vol. 13, no. 3, pp. 1499–1513, 2014.

[26] 3GPP TR 38.901, "Study on channel model for frequencies from 0.5 to 100 GHz," 2018.